Preprints of the 21st IFAC World Congress (Virtual)
Berlin, Germany, July 12-17, 2020

Autonomous Cascade Structure Feedback Controller Design With Genetic Algorithm-based Structure Optimization

Yoshihiro Maeda * **Shu Kunitate** * **Eitaro Kuroda** *
Makoto Iwasaki *

* *Department of Electrical and Mechanical Engineering, Nagoya Institute of Technology, Gokiso, Showa, Nagoya 4668555, Japan (email: ymaeda@nitech.ac.jp)*

Abstract: Designing a precise feedback (FB) controller that realizes the required properties such as a wide bandwidth and robust stability/sensitivity for resonant modes is a key design issue in achieving the fast and precise positioning performance of galvano scanners used in laser drilling. The aim of this study is to develop an efficient controller structure optimization method in an autonomous cascade structure FB controller design. The genetic algorithm efficiently searches the optimal structure for a target plant with high-order resonant modes in a short time according to the fitness of the controller parameter optimization problem. The effectiveness of the proposed method is demonstrated through a comparison with the conventional full search-based structure optimization method using a laboratory galvano scanner.

Keywords: Autonomous Design, Feedback Control, Cascade Structure, Gain/phase Stabilization, Fast and Precise Positioning, Galvano Scanner.

1. INTRODUCTION

Significantly fast and precise control of servo systems is required in industrial mechatronic systems such as electronics manufacturing machinery and machine tools for improved takt time and product quality (Iwasaki et al. (2012); Wu et al. (2011)). For instance, galvano scanners for printed circuit board (PCB) laser drilling machines perform thousands of point-to-point (PTP) positioning motions per second to make via holes on PCBs. The galvano scanner has mechanical resonant modes due to motor shaft torsion and galvano mirror deformation. Therefore, expanding the feedback (FB) control bandwidth while stabilizing the resonant modes is extremely difficult (Ito et al. (2017); Maeda et al. (2018)).

To design a wide bandwidth FB controller for such resonant servo systems, the gain/phase stabilization method (Nesline et al. (1985); Atsumi et al. (2005)) using second-order filters (such as notch, resonant, and all-pass filters) is often used as a valid approach in research fields. In this method, generally, a rigid mode compensator (such as a PID compensator) and some second-order filters are connected in series (cascade structure). These compensators and filters should be cooperatively designed to obtain a wide control bandwidth while robustly stabilizing the resonant modes. However, since its complex design procedure requires advanced technical skills for industrial engineers and researchers, advanced design techniques that can automatically design a FB controller are desirable.

In the gain/phase stabilization method-based FB controller design, the most important design problem for obtaining a precise FB controller is how to design an *optimal controller structure* with a combination of element compensators and parameters. Concerning the automatic design of controller parameters, several methods have been proposed in the literature, e.g., the convex optimization-based method (Iwasaki et al. (2005); Khatibi et al. (2008)), the nonlinear optimization-based method (Ibaraki et al. (2001); Maeda et al. (2018)), the meta-heuristics-based method (Krohling et al. (1997); Low et al. (2007)), and the experiment-based tuning method (Hamamoto et al. (2000); Maeda et al. (2019)). The above parameter design methods each have problems in that all cascade structure FB controller parameters cannot be designed owing to their nonlinear relationship, fine initial parameters close to the optimal ones that are needed, or a lengthy required design time. The studies on the automatic parameter design are currently being actively pursued. Conversely, there are few study examples on the design of *optimal controller structure*. The authors presented a full search-based structure optimization method (Kuroda et al. (2019)) as a basic approach. Although the conventional full search-based method can definitely obtain the optimum structure, the controller design time tends to be longer if there are many structural candidates.

In this study, an improved structure optimization method for a cascade structure FB controller is newly developed to shorten the controller design time. The proposed structure optimization method is based on the genetic algorithm (GA) (Tang et al. (1996)) since deterministic information about the structure optimization is not available in advance, and searches for the most suitable structure in less time by reducing the number of parameter optimization times for the non-optimal structure FB controllers. Therein, an associating operation between the structure

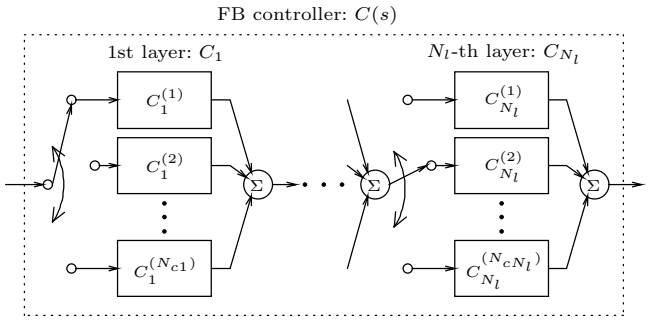

Fig. 1. Block diagram of an N_l-layer cascade structure FB controller (N_{cl} candidates for the l-th layer element compensator).

candidates and GA individuals, related to a parameter optimization fitness ranking, is presented as an effective search for the optimal structure. The effectiveness of the proposed method is demonstrated through the design example of a cascade structure FB controller for a laboratory galvano scanner, compared to the conventional full search-based method.

2. OPTIMAL FB CONTROLLER STRUCTURE SEARCH METHODS

2.1 Definition of a Cascade Structure FB Controller

A general expression of a single-input-single-output cascade structure FB controller is defined by (1) as a series connection of N_l element compensators.

$$C(s) = \prod_{l=1}^{N_l} C_l^{(n)}(s) \quad (n = \{1, 2, \ldots, N_{cl}\}), \tag{1}$$

where $C_l^{(n)}(s)$ means the n-th candidate of N_{cl} element compensators in the l-th layer and is defined as (2) with real undetermined coefficients $a_{kl}^{(n)}$ and $b_{kl}^{(n)}$ $(k = \{0, 1, 2\})$.

$$C_l^{(n)}(s) = \begin{cases} \dfrac{a_{2l}^{(1)}s^2 + a_{1l}^{(1)}s + a_{0l}^{(1)}}{b_{2l}^{(1)}s^2 + b_{1l}^{(1)}s + b_{0l}^{(1)}} \ (= C_l^{(1)}(s)) \\ \dfrac{a_{2l}^{(2)}s^2 + a_{1l}^{(2)}s + a_{0l}^{(2)}}{b_{2l}^{(2)}s^2 + b_{1l}^{(2)}s + b_{0l}^{(2)}} \ (= C_l^{(2)}(s)) \\ \quad \vdots \\ \dfrac{a_{2l}^{(N_{cl})}s^2 + a_{1l}^{(N_{cl})}s + a_{0l}^{(N_{cl})}}{b_{2l}^{(N_{cl})}s^2 + b_{1l}^{(N_{cl})}s + b_{0l}^{(N_{cl})}} \\ \qquad\qquad (= C_l^{(N_{cl})}(s)). \end{cases} \tag{2}$$

Fig. 1 shows a block diagram of $C(s)$ of (1). Since N_{cl} structure candidates are prepared for each layer, there are $N_{st} = \prod_{l=1}^{N_l} N_{cl}$ structure candidates in total as follows.

$$\mathcal{S}_{(1)}, \mathcal{S}_{(2)}, \cdots, \mathcal{S}_{(N_{st})}, \tag{3}$$

where $\mathcal{S}_{(\alpha)}$ $(\alpha = \{1, 2, \ldots, N_{st}\})$ expresses the symbols for N_{st} structure candidates and α is known as "structure number." The objective of this study is to efficiently determine the number α^* of the optimal structure $\mathcal{S}_{(\alpha^*)}$ (i.e., the optimal combination of the element compensators) that can obtain the widest control bandwidth with stabilizing resonant modes. Note that specific information about the promising structure candidates is unavailable (unknown) before starting an autonomous FB controller design.

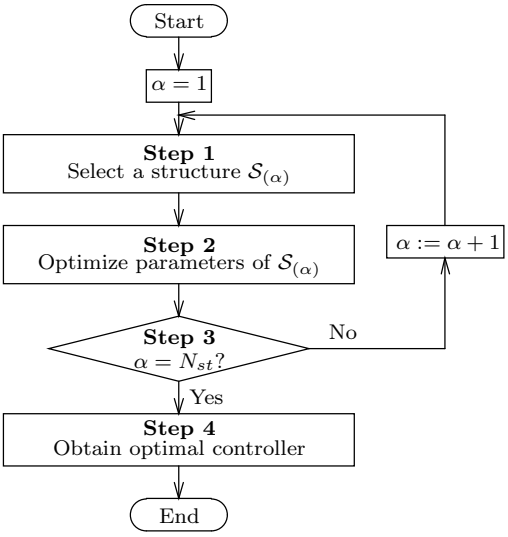

Fig. 2. Flowchart of the conventional automatic FB controller design using the full search-based structure optimization method.

2.2 Full Search-based Structure Optimization Method (Conventional Method)

Fig. 2 shows the flowchart of the conventional automatic cascade structure FB controller design with the full search-based structure optimization approach. The design procedure is briefly summarized as follows.

Step 1 A structure candidate $\mathcal{S}_{(\alpha)}$ whose structure number is α and parameters are not optimized is selected.

Step 2 Parameters $a_{kl}^{(n)}$ and $b_{kl}^{(n)}$ of the selected structure are designed using the cooperative optimization algorithm (Maeda et al. (2018)) and the fitness $\mathcal{F}_{(\alpha)}$ concerning the control bandwidth is obtained. Here, the cooperative optimization algorithm requires N-time iterative calculations for obtaining sufficiently converged parameters.

Step 3 If α is less than N_{st}, then make $\alpha := \alpha + 1$ and return to Step 1. Else, go to Step 4.

Step 4 The number α^* of the optimal structure is determined according to the following optimization problem.

$$\alpha^* = \arg\min_{\alpha} \ \{\mathcal{F}_{(1)}, \mathcal{F}_{(2)}, \ldots, \mathcal{F}_{(N_{st})}\}. \tag{4}$$

By performing the above steps, the most suitable FB controller (i.e., not only optimal structure $\mathcal{S}_{(\alpha^*)}$ but also its parameters) can be designed automatically (Kuroda et al. (2019)). However, since the conventional method should optimize controller parameters for all structure candidates (i.e., $N_{st}N$-time iterations are required), the controller design time tends to be longer when there are numerous structure candidates. Therefore, in the next section, an improved structure optimization method that selectively optimizes optimal structure parameters is newly proposed to shorten the design time.

2.3 GA-based Structure Optimization Method (Proposed Method)

In the proposed controller structure optimization method, the optimal structure is searched by a GA (Tang et al. (1996)) using the ranking numbers $\beta = \{1, 2, \ldots, N_{st}\}$.

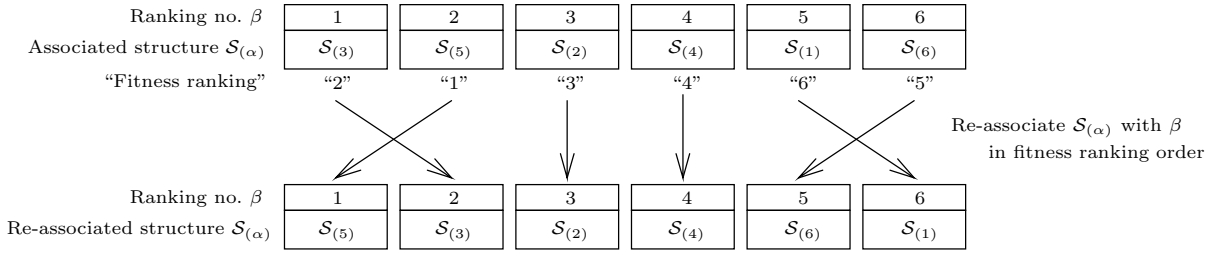

Fig. 4. Concept of the re-associating operation (sample case of $N_{st} = 6$).

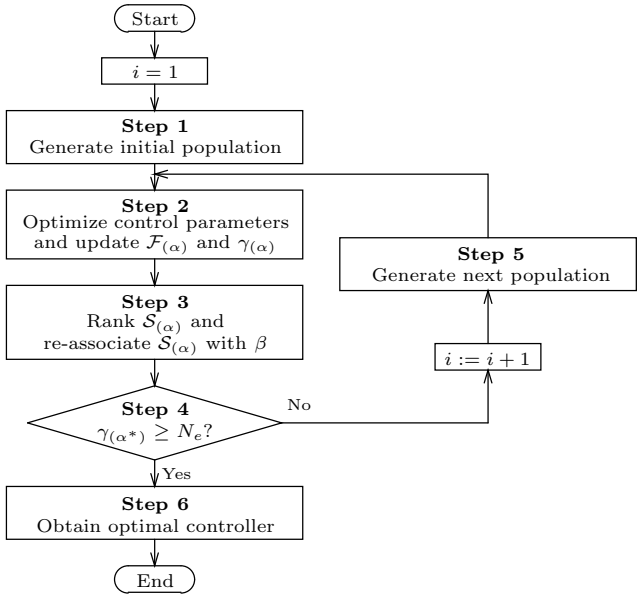

Fig. 3. Flowchart of the proposed autonomous FB controller design using the GA-based structure optimization method.

Each ranking number is associated with a structure candidate in $\mathcal{S}_{(\alpha)}$ and β is considered as a GA individual. The notable point is that the parameter optimization for one individual in each generation is performed in fewer iterations and the optimal structure parameters are selectively optimized by the GA. Fig. 3 shows the flowchart of the proposed autonomous FB controller design method using the GA-based structure search method, and the procedure is detailed as follows.

Step 1 The initial population that includes all numbers of β as the individuals is generated (N_{ind} individuals in a population).

Step 2 Parameters $a_{kl}^{(n)}$ and $b_{kl}^{(n)}$ are optimized for each individual (structure candidate) using the cooperative optimization algorithm (Maeda et al. (2018)). Next, the elite fitness $\mathcal{F}_{(\alpha)}$ and the selected number of times $\gamma_{(\alpha)}$ of all structure candidates are updated, according to the parameter optimization results. Here, if $i \geq 2$, then the parameter optimization starts from the elite parameters until the last generation as the initial parameters. Note that the iteration number of times N_{para} of the cooperative optimization for each individual is set to a lower number than N ($N_{para} < N$). In addition, if there are M ($M \geq 2$) individuals with the same structure in the current population, then MN_{para} iterations are performed on the corresponding structure candidate.

Step 3 All structure candidates of $\mathcal{S}_{(\alpha)}$ are ranked according to the latest fitness and then are re-associated with $\beta = 1$ to $\beta = N_{st}$ in the ranking order. Fig. 4 shows the concept of the re-associating operation. By performing the re-associating operation, the structure candidates are sorted in the promising order. As a result, the promising structures (individuals) can be selected in the next population generation.

Step 4 If $\gamma_{(\alpha^*)}$ of the best-ranking structure (i.e., $\beta = 1$) satisfies $\gamma_{(\alpha^*)} \geq N_e$, then go to Step 6. Else, go to Step 5. Here, N_e is the upper limit of the selected number of times as the end condition ($N = N_{para}N_e$), which ensures N iterations of the parameter optimization only for the optimal structure $\mathcal{S}_{(\alpha^*)}$.

Step 5 The genetic operations such as selection, crossover, and mutation are done for the re-associated individuals β and generate a new population. After that, return to Step 2. The equivalent optimization problem of the GA that searches the optimal structure is defined by (5),

$$\min_{\beta} \ \mathcal{F}_{(\alpha^*)}. \tag{5}$$

Step 6 A FB controller that has the best-ranking number $\beta = 1$ is selected as the optimal FB controller whose structure number is α^*.

In the proposed GA-based structure search, the promising structure candidates possess plural individuals in each generation and the parameter optimization is iteratively performed for them. As a result, the controller design time is shortened compared to the conventional method.

3. GALVANO SCANNER AND ITS CONTROL SYSTEM

3.1 Galvano Scanner

The laboratory galvano scanner used as a target servo system in this study is shown in Fig. 5. For a detailed explanation of the galvano scanner mechanism and control system, see the reference (Maeda et al. (2015)). The black broken lines in Fig. 6 show an experimental bode plot of the motor angle θ_m from the motor current reference i_{ref} as the control input. There exist some resonant modes due to motor shaft torsion and galvano mirror deformation, i.e., the first resonant mode at 2.98 kHz, the second resonant mode at 5.96 kHz, and the high-order resonant modes over 10 kHz. To model the resonant characteristics, the following equation is introduced as the plant model.

$$P(s) = Ke^{-Ls}\left(\frac{1}{s^2} + \sum_{i=1}^{6} \frac{k_i}{s^2 + 2\zeta_i\omega_i s + \omega_i^2}\right), \tag{6}$$

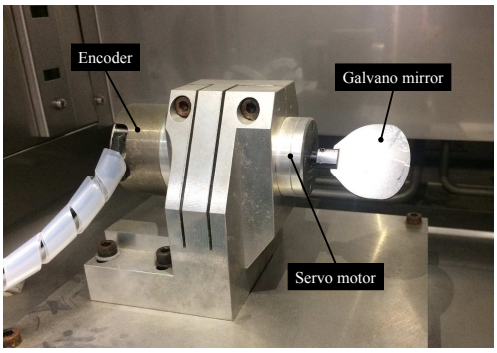

Fig. 5. Exterior of the laboratory galvano scanner.

where K is the gain considering the moment of inertia J, the motor torque constant K_t, and the steady gain of the current control system K_c, L is the equivalent dead time, ω_i is the natural angular frequency of the i-th resonant mode, ζ_i is the damping coefficient, and k_i is the resonant mode gain. The parameters of $P(s)$ is identified by the nonlinear least squares method. The blue solid lines in Fig. 6 are the bode plot of $P(s)$.

To realize the fast and precise positioning performance, the wide-bandwidth FB control with the robustly stabilized resonant modes is necessary. Therefore, a gain margin of 5 dB and a phase margin of 30 deg should be satisfied as the stability specifications, while sensitivity gains of -20 dB and -10 dB at the first and second resonant frequencies should be ensured as the sensitivity specifications for obtaining precise vibration suppression properties.

3.2 Positioning Control System

A block diagram of the two-degree-of-freedom (2DoF) control system for the galvano scanner is shown in Fig. 7, where $F_{ff}(z)$ is the deadbeat feedforward (FF) controller (Maeda et al. (2015)), $P_n(z)$ is the discrete-time plant model, $C(z)$ is the FB controller, u_{ff} is the FF control input, $u(= i_{ref})$ is the control input, r_c is the target position (step signal), r is the position trajectory reference, and $y(\propto \theta_m)$ is the motor position. $P_n(z)$ which corresponds to the design model for $F_{ff}(z)$ is the discretized model of $P(s)$ in (6) without the fourth to sixth resonant modes.

On the other hand, $C(z)$ is designed as a cascade structure FB controller using a PID compensator for the rigid mode and two second-order filters for the first and second resonant modes. The mathematical expression of $C(z)$ is defined by (7) in the continuous-time domain.

$$\begin{aligned} C(s) &= C_{PID}(s)\prod_{q=1}^{2} C_{Rq}(s) \\ C_{PID}(s) &= K_P + \frac{K_I}{s} + \frac{K_D s}{T_D s + 1} \\ C_{Rq}(s) &= \frac{s^2 + 2\zeta_{Rnq}\omega_{Rq}s + \omega_{Rq}^2}{s^2 + 2\zeta_{Rdq}\omega_{Rq}s + \omega_{Rq}^2}, \end{aligned} \tag{7}$$

where $C_{PID}(s)$ is the PID compensator and $C_{Rq}(s)$ is the notch filter (NF) or the all-pass filter (APF). $C_{Rq}(s)$ is designed based on the gain/phase stabilization method (Nesline et al. (1985); Atsumi et al. (2005)) to shape the target resonant modes. On the other hand, $C_{PID}(s)$

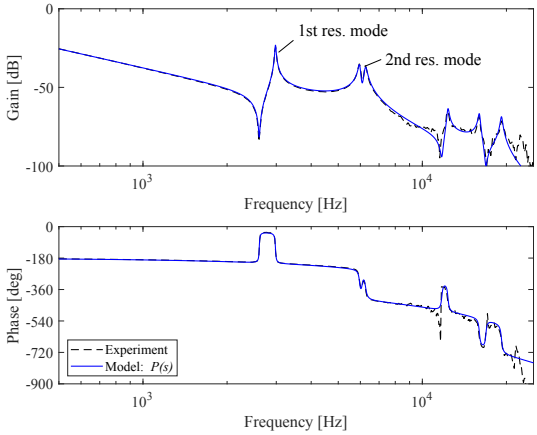

Fig. 6. Bode plots of the galvano scanner.

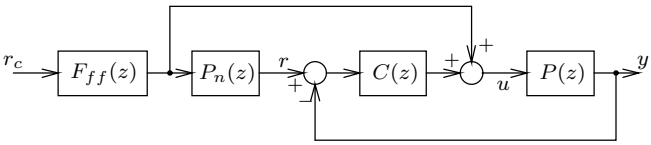

Fig. 7. Block diagram of the 2DoF positioning control system.

is designed for expanding the control bandwidth. The parameters $\rho = \{K_P, K_I, K_D, T_D, \zeta_{Rn1}, \omega_{Rd1}, \zeta_{Rn2}, \omega_{Rd2}\}$ should be cooperatively designed considering the balance of control bandwidth, stability margins, and sensitivity, which requires considerable labor and/or expert skills in the manual design.

4. EVALUATIONS OF AUTONOMOUS FB CONTROLLER DESIGN METHODS

4.1 Settings of Autonomous FB Controller Design

The proposed and conventional FB controller structure optimization methods are applied to the design problem of a cascade structure FB controller expressed by (7) for the galvano scanner.

The target plant was considered as (6), and FB controller structure candidates were prepared as follows.

- $N_l = 3$ layers.
- $N_{c1} = 1$ element compensator for the first layer as a PID compensator.
- $N_{c2} = N_{c3} = 3$ element compensators for the second and third layers as a unit gain (Gain), a NF, and an APF.

In the third term, selecting the unit gain means that the gain/phase stabilization method is not applied to the target resonant mode. Therefore, the total number of structure candidates becomes $N_{st} = N_{c1}N_{c2}N_{c3} = 9$.

In the cooperative optimization-based parameter optimization method, circular conditions for ensuring the specified stability margins and sensitivity gains around the first and second resonant frequencies as stated in 3.1 were considered as inequality constraints of $\mathcal{R}_{sta}(\rho) > 0$ and $\mathcal{R}_{sen}(\rho) > 0$, respectively. In addition, the objective function $\mathcal{J}_{sen}(\rho)$ that evaluates errors between the desired

Table 1. Parameters of the GA.

Individual number	18	Selection method	Tournament
Crossover rate	0.9	Crossover method	Single point
Mutation rate	0.01		

Table 2. FB controller design results: fitness of parameter optimization; characteristic indices of frequency response; PTP positioning performance.

Method	Structure	Fitness	Remarks	BW [Hz]	GM [dB]	PM [deg]	SG1 [dB]	SG2 [dB]	MAE [μm]	RMSE [μm]
Conv. (Full-search)	PID-Gain-Gain	2×10^{14}	No feasible solution	261	12.5 (4540 Hz)	32.4 (3060 Hz)	$-14.8^{\dagger}$	$-7.0^{\dagger}$	4.94	2.97
	PID-Gain-NF	1×10^{14}	↑	341	6.0 (4769 Hz)	34.4 (3179 Hz)	-20.4	$-3.1^{\dagger}$	4.48	2.27
	PID-Gain-APF	1×10^{14}	↑	401	5.9 (6831 Hz)	34.5 (3119 Hz)	$-18.3^{\dagger}$	-12.5	4.94	2.63
	PID-NF-Gain	1×10^{14}	↑	601	6.6 (4017 Hz)	30.4 (986 Hz)	$-13.3^{\dagger}$	-11.8	4.94	1.78
	PID-NF-NF	456		562	6.1 (4376 Hz)	30.3 (933 Hz)	-20.5	-10.3	4.94	1.87
	PID-NF-APF	9905		407	5.9 (4204 Hz)	30.3 (765 Hz)	-20.1	-14.1	6.30	2.59
	PID-APF-Gain	1635		536	6.8 (2808 Hz)	30.3 (909 Hz)	-21.2	-11.2	4.94	2.00
	PID-APF-NF	198	Optimal	562	6.1 (4393 Hz)	30.4 (926 Hz)	-22.3	-10.2	4.94	1.88
	PID-APF-APF	2017		527	6.4 (4232 Hz)	30.3 (900 Hz)	-21.7	-12.3	5.39	2.34
Proposed (GA)	PID-APF-NF	122	Optimal	595	6.2 (4373 Hz)	30.4 (982 Hz)	-22.5	-10.1	4.93	1.80

sensitivity characteristic and the actual one at low frequencies was utilized to obtain a wide control bandwidth. The equivalent optimization problem of the parameter design is expressed as follows.

$$\begin{aligned} \rho^* &= \arg\min_{\rho} \ \mathcal{J}_{sen}(\rho) \\ &\text{s.t. } \mathcal{R}_{sta}(\rho) > 0, \ \mathcal{R}_{sen}(\rho) > 0. \end{aligned} \tag{8}$$

For more parameter optimization method details, see the reference (Maeda et al. (2018)).

In the conventional full search-based structure optimization method, the iteration number of times N of the parameter optimization for each structure candidate was set to $N = 1000$, since at least 1000 iterations are needed to determine sufficiently converged parameters. On the other hand, in the proposed GA-based structure optimization method, the iteration number of times N_{para} of the parameter optimization was chosen as $N_{para} = 5$ and the end condition was set to $N_e = 200$ to satisfy $N_{para}N_e = N$. The setting parameters of the GA are listed in Table 1. In this study, 2 individuals for each structure candidate were selected in the initial population as the individual number N_{ind} was chosen as $N_{ind} = 2N_{para} = 18$.

4.2 Evaluations of Fitness and Design Time

The fitness $\mathcal{F}_{(\alpha)}$ in the conventional method and the best-ranking fitness $\mathcal{F}_{(\alpha^*)}$ of the optimal structure in the proposed method are listed in Table 2. The conventional method selected "PID-APF-NF" (i.e., a PID compensator for the rigid mode, an APF for the first resonant mode, and a NF for the second resonant mode) as the optimal structure from 9 structure candidates. On the other hand, the proposed method successfully obtained the same "PID-APF-NF" as the optimal structure.

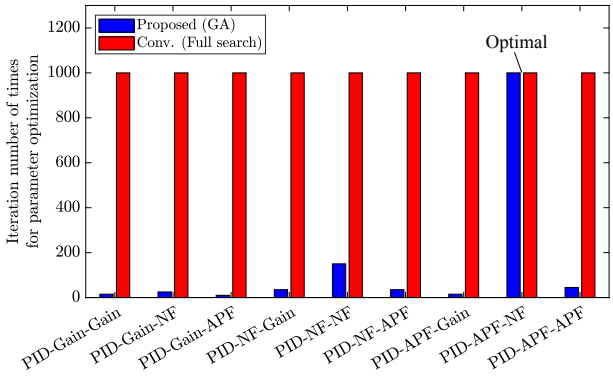

Fig. 8. Comparison of number of iterations for parameter optimization.

Fig. 8 shows the number of iterations for parameter optimization of all structure candidates. Although the conventional method performed $N_{st}N = 9000$ iterations in total for obtaining the optimal structure, the proposed method reduced the total number of iterations to 1330 by selectively optimizing the optimal structure candidate by the GA. As a result, the proposed method shortened the design time from 23913 s obtained by using the conventional method to 3573 s, an 85 % improvement.

4.3 Evaluations of Frequency Characteristics

The FB control systems designed by the proposed and conventional methods are comparatively evaluated in the frequency domain. The frequency characteristics of the obtained FB control systems are shown in Fig. 9, where blue solid lines indicate the proposed method results, red solid lines represent the optimal structure obtained by the conventional method, and red dotted lines represent the

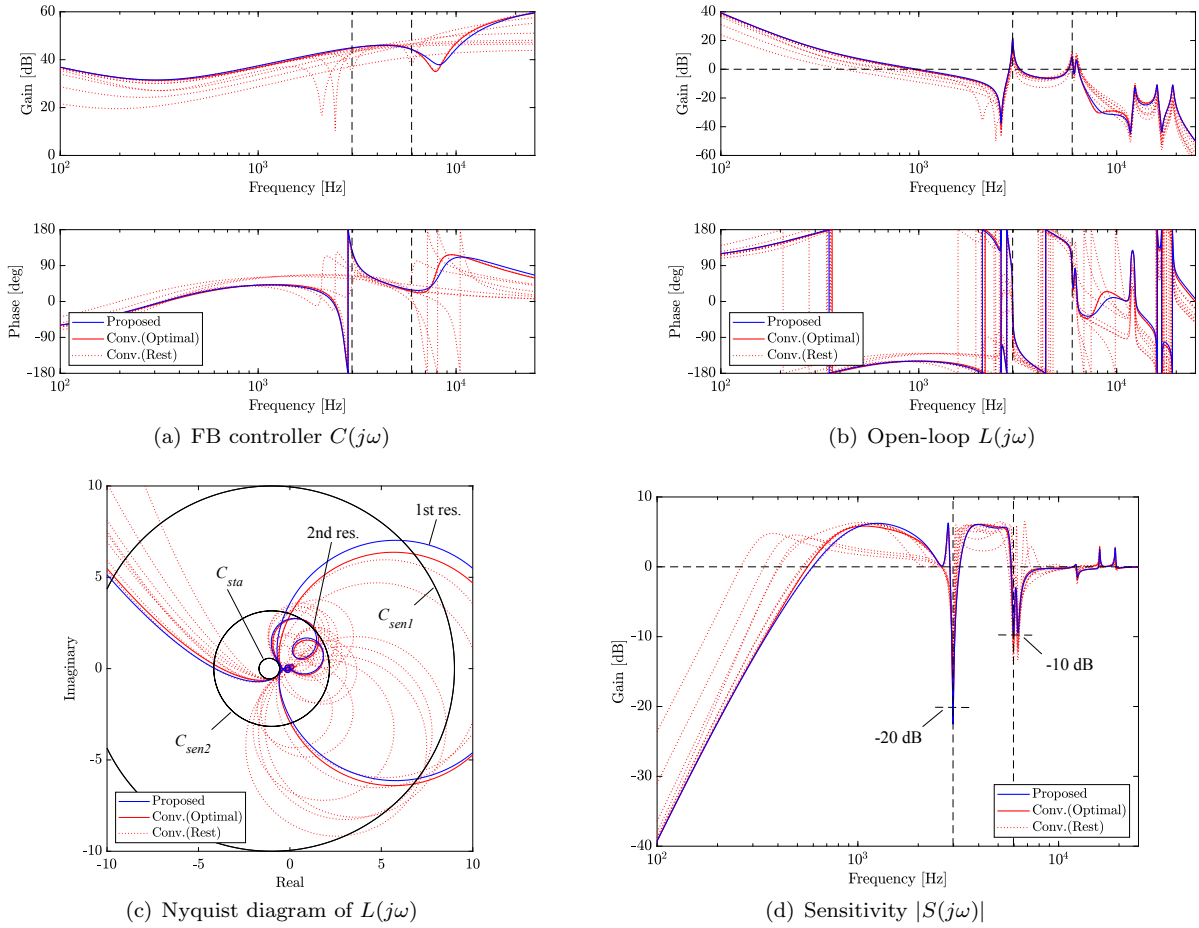

(a) FB controller $C(j\omega)$

(b) Open-loop $L(j\omega)$

(c) Nyquist diagram of $L(j\omega)$

(d) Sensitivity $|S(j\omega)|$

Fig. 9. Frequency characteristics of FB control system: (a) FB controller $C(j\omega)$; (b) open-loop characteristic $L(j\omega)$; (c) Nyquist diagram of $L(j\omega)$; (d) sensitivity characteristic $|S(j\omega)|$.

other structure candidates obtained by the conventional method. From Fig. 9(a), the proposed method obtained almost the same controller properties as of the conventional method, since the same structure was selected and the same number of iterations were performed in the parameter optimization. The optimal FB controller obtained higher gains at low frequencies in all structure candidates as shown in Fig. 9(a) and Fig. 9(b). Conversely, owing to the gain/phase stabilization-based design of $C_{R1}(s)$ and $C_{R2}(s)$ for the first and second resonant modes, the Nyquist trajectory ensured the desired stability margins of 5 dB and 30 deg specified by the circle C_{sta} in Fig. 9(c) while attenuating the sensitivity gains at the first and second resonant frequencies to less than -20 dB and -10 dB, respectively, in Fig. 9(d) (the circles C_{sen1} and C_{sen2} in Fig. 9(c) represent the sensitivity gain constraints). Note that sufficient robust stability against the first and second resonance frequency variations was ensured by imposing the sensitivity gain constraints, although the obtained NF and APF had sharp gain and phase properties around the resonant modes.

As a quantitative evaluation result of the frequency characteristics, control bandwidth (BW) defined as the lowest zero crossing frequency of the sensitivity characteristic in this study, gain margin (GM), phase margin (PM), sensitivity gain at the first resonant frequency (SG1), and sensitivity gain at the second resonant frequency (SG2) are summarized in Table 2. Note that the mark † on SG1 and SG2 denotes that the corresponding sensitivity constraint was not satisfied in the parameter optimization (i.e., no feasible solution), and 4 structure candidates without feasible solution (PID-Gain-Gain, PID-Gain-NF, PID-Gain-APF, and PID-NF-Gain) cannot be used as a FB controller. It has been confirmed that the proposed method successfully obtained the widest BW while ensuring almost same GM, PM, SG1, and SG2 as of the remaining 5 structure candidates (PID-NF-NF, PID-NF-APF, PID-APF-Gain, PID-APF-NF, and PID-APF-APF) of the conventional method.

4.4 Evaluations of PTP Positioning Performance

Fig. 10 shows the simulated response waveforms of the position tracking error $r - y$ for $r_c = 1$ mm stroke PTP positioning motion with the target settling time of 0.72 ms, using the 2DoF position control system of Fig. 7. In the simulations, the torque constant K_t in $P(s)$ of (6) were intentionally varied by 1 % from the nominal value, assuming the effects of temperature variations due to environment and self-heating (Maeda et al. (2015)). From Fig. 10, it can be recognized that the controller structure significantly affected the position tracking accuracy during the transient and after the target settling time of 0.72 ms indicated by a vertical black dashed line. The maximum absolute error (MAE) and the root mean square error (RMSE) at 0.72 ms to 3 ms for each designed FB controller are listed

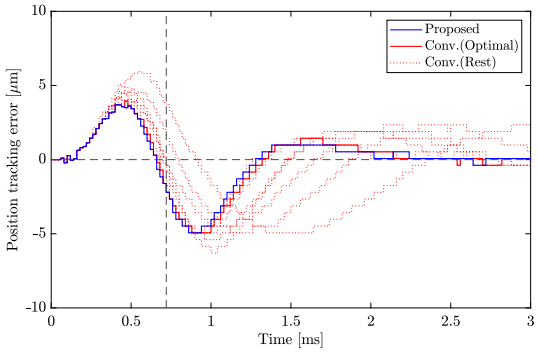

Fig. 10. Position tracking errors using the designed FB controllers in 1 mm stroke PTP positioning.

in Table 2. The position tracking performance specifically had a correlation with the parameter optimization fitness and the control bandwidth (BW), and the optimal FB controller designed by the proposed method obtained the best position tracking performance of all the evaluated FB controllers.

From the series of evaluations described in Sections 4.2 $\sim$ 4.4, it has been verified that the proposed GA-based optimal controller structure search method could design a wide-bandwidth FB controller with shorter design time than the conventional full search-based method. Note that the autonomous cascade structure FB controller design using the proposed structure search method was performed 30 times for evaluating its reproductivity, and as a result, the same optimal structure (PID-APF-NF) and almost same parameters were successfully obtained in all design results.

5. CONCLUSION

An autonomous cascade structure FB controller design method using the proposed GA-based optimal structure search approach is developed. The proposed method optimizes controller structure and parameters that obtain the widest control bandwidth by stabilizing high-order resonant modes in less time than the conventional full search-based structure optimization method. In addition, it is demonstrated that the optimal FB controller designed using the proposed method achieves the most suitable fast and precise positioning performance compared to other structure FB controllers.

ACKNOWLEDGMENT

The authors would like to thank Via Mechanics, Ltd, for providing the required experimental equipment.

REFERENCES

Atsumi, T., Arisaka, T., Shimizu, T., and Masuda, H. (2005). Head-positioning control using resonant modes in hard disk drives. *IEEE/ASME Transactions on Mechatronics*, 10(4), 32–40.

Hamamoto, K., Fukuda, T., and Sugie, T. (2000). Iterative feedback tuning of controllers for a two-mass spring system with friction. In *Proceedings of the 39th IEEE International Conference on Decision and Control*, 2438–2443.

Ibaraki, S. and Tomizuka, M. (2001). High precision motion control techniques –A promising approach to improving motion performance. *Journal of Dynamic Systems, Measurement and Control*, 123(3), 544–549.

Ito, S., Yoo, H.W., and Schitter, G. (2017). Comparison of modeling-free learning control algorithms for galvanometer scanner's periodic motion. In *Proceedings of the 2017 IEEE International Conference on Advanced Intelligent Mechatronics*, 1357–1362.

Iwasaki, M., Seki, K., and Maeda, Y. (2012). High precision motion control techniques –A promising approach to improving motion performance. *IEEE Industrial Electronics Magazine*, 6(1), 32–40.

Iwasaki, T. and Hara, S. (2005). Generalized KYP lemma: Unified frequency domain inequalities with design applications. *IEEE Transactions Automatic Control*, 50(1), 41–59.

Khatibi, H., Karimi, A., and Longchamp, R. (2008). Fixed-order controller design for polytopic systems using LMIs. *IEEE Transactions on Automatic Control*, 53(1), 428–434.

Krohling, R.A., Jaschek, H., and Rey, J.P. (1997). Designing PI/PID controllers for a motion control system based on genetic algorithms. In *Proceedings of the 12th IEEE International Symposium on Intelligent Control*, 10.1109/ISIC.1997.626429.

Kuroda, E., Maeda, Y., and Iwasaki, M. (2019). An autonomous design method of a cascade structure feedback controller. In *Proceedings of the 8th IFAC Symposium on Mechatronic Systems*, 808–813.

Low, K.-S. and Wong, T.-S. (2007). A multiobjective genetic algorithm for optimizing the performance of hard disk drive motion control system. *IEEE Transactions on Industrial Electronics*, 54(3), 1716–1725.

Maeda, Y. and Iwasaki, M. (2015). Improvement of adaptive property by adaptive deadbeat feedforward compensation without convex optimization. *IEEE Transactions on Industrial Electronics*, 62(1), 466–474.

Maeda, Y., Kuroda, E., Uchizono, T., and Iwasaki, M. (2018). Hybrid Optimization Method for High-performance Cascade Structure Feedback Controller Design. In *Proceedings of the 44th Annual Conference of the IEEE Industrial Electronics Society*, 4588–4593.

Maeda, Y., Gou, N., and Iwasaki, M. (2019). A Stable Parameter Area Calculation Method for Advanced Auto-tuning of a Feedback Controller. In *Proceedings of the 17th IEEE International Conference on Industrial Informatics*, 541–546.

Nesline, F.W. and Nesline, M.L. (1985). Phase vs. gain stabilization of structural feedback oscillations in homing missile autopilots. In *Proceedings of the 1985 American Control Conference*, 323–329.

Tang, K.S., Man, K.F., and Gu, D.-W. (1996). Structured genetic algorithm for robust H_∞ control systems design. *IEEE Transactions on Industrial Electronics*, 43(5), 575–582.

Wu, J., Xiong, Z., Lee., K.-M., and Ding, H. (2011). High-acceleration precision point-to-point motion control with look-ahead properties. *IEEE Transactions on Industrial Electronics*, 58(9), 4343–4352.